32nd European Modeling & Simulation Symposium
17th International Multidisciplinary Modeling & Simulation Multiconference

ISSN 2724-0029 ISBN 978-88-85741-44-7 © 2020 The Authors.
DOI: 10.46354/i3m.2020.emss.052

Integrated Contra-Directional Coupler for NV-centers photon filtering

Anna Elmanova[1*], Ilia Elmanov[1], Vadim Kovalyuk[1], Pavel An[1] and Gregory Goltsman[1,2]

[1]Department of Physics, Moscow State Pedagogical University, 119435, Russia
[2]National Research University Higher School of Economics, Moscow 101000, Russia

[*]Corresponding author. Email address: anna.elmanova.belskaya@gmail.com

Abstract

We modelled an integrated optical contra-directional coupler on silicon nitride platform. Performance of the filter was studied depending on different parameters, including the grating period and the height of teeth of the Bragg grating near 637 nm operation wavelength. The obtained results can be used for a design and fabrication of quantum photonic integrated circuits with on-chip single-photon NV-centers in nanodiamonds.

Keywords: Quantum photonic integrated circuit, Contra-Direction Coupler; On-chip Bragg filter; NV-center

1. Introduction

Photon integrated circuits (PICs) are widely used in modern scientific and technical applications, while their full potential has not yet been revealed. For example, PICs are used in communication systems and signal processing (Wang, Shi, Vafaei, Jaeger & Chrostowski, 2011), spectroscopy, biosensing (De Vos, Bartolozz, Schacht, Bienstman & Baets, 2007), quantum communications and so on. Among the new and potential applications, the quantum ones (quantum simulations, computing) can take computing to a whole new level (O'Brien, 2007).

Quantum-PICs (QPICs) developed for the needs of linear optical quantum computing (LOQQ) should include passive optical elements, single-photon sources, and single-photon detectors (Aspuru-Guzik & Walther 2012). A few years ago, it was demonstrated the first single-photon detector integrated into QPICs. It was based on superconducting single-photon detector and showed high quantum efficiency - close to 100% and low dark counts rate down to 1Hz (Ferrari, Schuck & Pernice, 2018). In the present time, the creation of ideal on-chip single-photon sources is still an actual task. Such sources, on the one hand, should emit indistinguishable single photons on demand, and on the other hand, emitted photons should be separated from the powerful optical pumping.

Due to a number of advantages, one of the promising candidates for on-chip single-photon source is a nitrogen-vacancy (NV) in diamond, which efficiently emits photons in zero phonon line at 637 nm wavelength (Bahe et al., 2009). Such sources can operate at room temperatures and have a high coherence time (Aharonovich et al., 2011). Although nanodiamonds with NV-centers can be placed in a controlled manner atop of a photonic integrated platform by using e-beam lithography (Komrakova, Javadzade, Vorobyov & Bolshedvorskii, 2019), an important issue related to on-chip pump rejection should be investigated.

As a material for the integrated device study, we chose silicon nitride. Among different photonic integrated platforms, such as silicon-on-insulator (SOI), silica, gallium arsenide, indium phosphide, etc., silicon nitride (Si_3N_4) has wide bandgap (~5eV) (Silverstone, Bonneau, O'Brien & Thompson, 2016) allowing to operate in visible and near-infrared wavelength ranges (Doerr, 2015) with minimal optical losses (Soref, 2006). Optical losses play an important role in QPICs and significantly limit the creation of scalable on-chip QPICs at present. At the same time, NV-centers emit in the visible range, where silicon does not transmit light. Thus, the SiN-platform has a great advantage for the creation of QPICs.

In this article, to solve the pump rejection problem for the splitting pump and photons emitted by NV-centers, we modeled of a nanophotonics contra-directional coupler (CDC), based on the corrugated Bragg waveguide (Wang, Shi & Chrostowski, 2013). Such device operates similar to selective mirrors for some part of the spectrum, where most of the non-reflected light goes through the structure (Yeh & Taylor, 1980).

2. State-of-the-art

Periodic changes in the refraction coefficient of the material can be used to introduce conditions for the selective light pass (Bragg's conditions). For integrated photonic circuits, the simplest way to introduce such changes is the creation of the corrugated waveguide with a number of "teeth". (Shi et al., 2012).

Bragg gratings have a number of advantages, such as precise design in order to obtain the desired values for spectral selectivity (full width on half maximum, FWHM), notch wavelength and the efficiency (depth) of the filtration. However, the disadvantage of such grating, the radiation reflects back to the input port. Contra-directional Bragg gratings conserve most of the properties of the usual Bragg gratings, but at the same time due to the separation of input and output waveguides, one can work as an optical circulator. The geometry of contra-directional couplers includes two waveguides on a small distance from each other, whereby, the radiation can pass from one waveguide to another. These waveguides have different widths and the light at a reflected wavelength is directed to the opposite direction relatively to the incident. Besides, asymmetrical geometry of the waveguides the filter performance, including free spectral range (FSR) and optical isolation can be improved also (Yves, 2017).

Recently, quite extensive research has been carried out on the modeling of Bragg waveguides on different platforms. In addition to the above platforms used for PICs, some of exotic ones, like polymeric contra-directional Bragg gratings (Chuang, Huang, Lin, & Lee, 2011) or contra-directional filter with metamaterial slab (Topa, 2002) were demonstrated.

In the article (Naghdi & Chen, 2016) for numerical simulation of an asymmetric filter on SOI platform a finite difference time domain (FDTD) method in a 3D was used. The filter contained the rectilinear waveguide and the Bragg grating. The authors introduced a filter with notch wavelength of 1550-1560 nm and investigated the dependence of FWHM from the distance between the two waveguides. The work is important due to the precision of the FDTD method, predicting the spectral picture obtained experimentally.

A similar task was fulfilled by the authors of an article (Siregar, Bahtiar, Abrar, 2007). Here the Bragg waveguide is also combined with a rectilinear one. In the article, the spectra for transmission and reflection are fully calculated numerically without simulations. In another article (Okayama et al., 2019) we can see another combination of a rectilinear waveguide with contra-directed Bragg one. The main peak of the filter had the FWHM equal to 6 nm and operated near to 1600-1610 nm wavelengths. The simulations were carried out using the 3D FDTD method.

There is a paper about development of the contra-directional Bragg filter on SOI platform with two Bragg gratings of different periods (Boroojerdi, Ménard, & Kirk, 2016). Here the authors used mode expansion method (EME) solver from Lumerical to simulate filter performance. Although it was developed for wavelength of 1540 and 1560 nm, experiment showed the shift of the central wavelengths up to 1550 and 1570 nm, correspondingly.

In the article (Zubkova et al., 2018) a contra-directional filter on Si_3N_4 platform was studied. The design for the notch wavelength of 1550 nm was calculated using the finite element method (FEM) in COMSOL Multiphysics. In order to obtain a single-mode regime, the waveguide widths and effective refractive indexes were calculated numerically, and Bragg grating period found analytically. After fabrication and measurements, a linear dependence of the central wavelength on the grating period were found in a good agreement with calculated results.

Similar to our research material and spectral range were introduced in the article (Nie, Turk, Liu, & Baets, 2019), where the contra-directional Bragg filter on Si_3N_4 platform with notch wavelength 789 nm and FWHM 1.7 nm was demonstrated.

The authors used FIMMWAVE to perform a cross-sectional simulation and a theoretical calculation and obtain the parameters of the filter. We used this work as a starting point for our research.

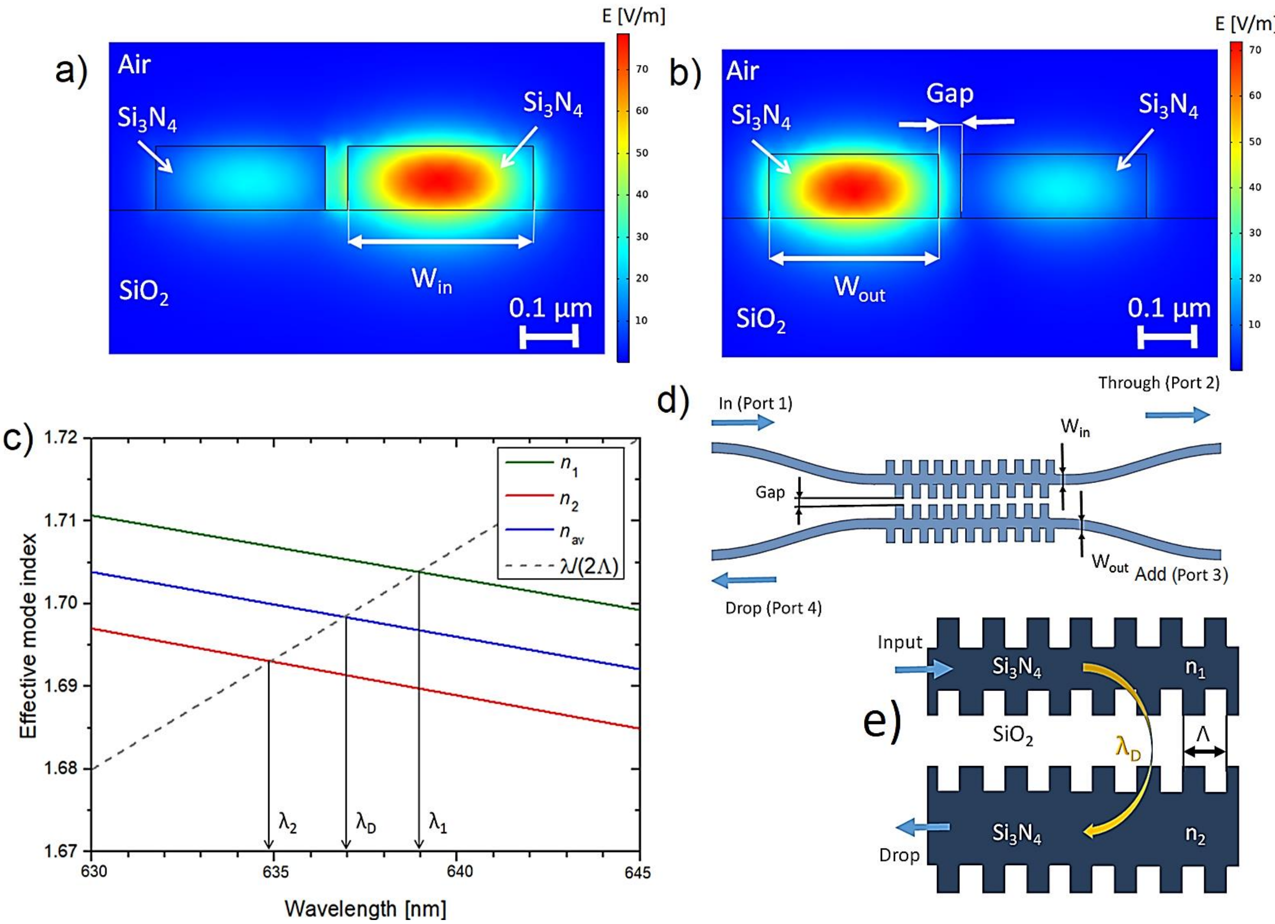

Figure 1. a) COMSOL simulation for the cross-sectional electrical field distribution inside the CDC waveguides for the first mode. b) The same for the second mode. c) Calculated spectra of the effective mode indices for both modes. Phase matched wavelengths are indicated by arrows. d) Schematically depicted contra-directional coupler based on the Bragg grating. Directions of the input and the output light, as well as all of the ports are shown. The widths of the waveguides and the gap between them are marked. e) The light propagation at peak wavelength is schematically depicted by a yellow arrow. The input and output ports are depicted with blue arrows.

All the articles listed above are good examples of different asymmetrical filters based on Bragg gratings. We used this experience to perform our task for design creation of an efficient contra-directional filter for notch wavelength of 637 nm.

3. Materials and Methods

For the numerically studied model we used parameters of the commercially available silicon nitride wafers with thermal silicon oxide SiO_2 = 2 µm and silicon nitride Si_3N_4 = 200 nm layers atop. The spectral dependence of refractive indices for SiO_2 were taken from (Malitson, 1965) and for Si_3N_4 from (Philipp, 1973). To achieve the conditions for total internal reflection, the Si_3N_4 waveguiding layer (n = 2.01 @ 637 nm) was covered by air (n = 1) from above and SiO_2 (n = 1.4569 @ 637 nm) from below. The device design consisted of two separated Bragg contra-directional gratings and the four optical ports (input, through, add and drop) (Figure 1d,e).

To find the required optical parameters of the Bragg waveguides, we optimized the design of CDC, including period, filling factor, number of periods, the height of "teeth", as well as the waveguides widths and the gap.

We used the finite element method in COMSOL Multiphysics and finite difference time domain method in MEEP to obtain effective mode indexes, as well as reflection and transmission spectra through the CDC, respectively. COMSOL was solving Maxwell equations (Ghose, 2010), and MEEP was solving Green's tensors (Oskooi, 2010). We determined the radiation source as a dipole atop of one of the ports in order to represent NV-centers correctly.

We calculated the transmission and reflection of the filter using this model. For computations, we used a wave package consisting of 1300 different frequencies propagated over the filter.

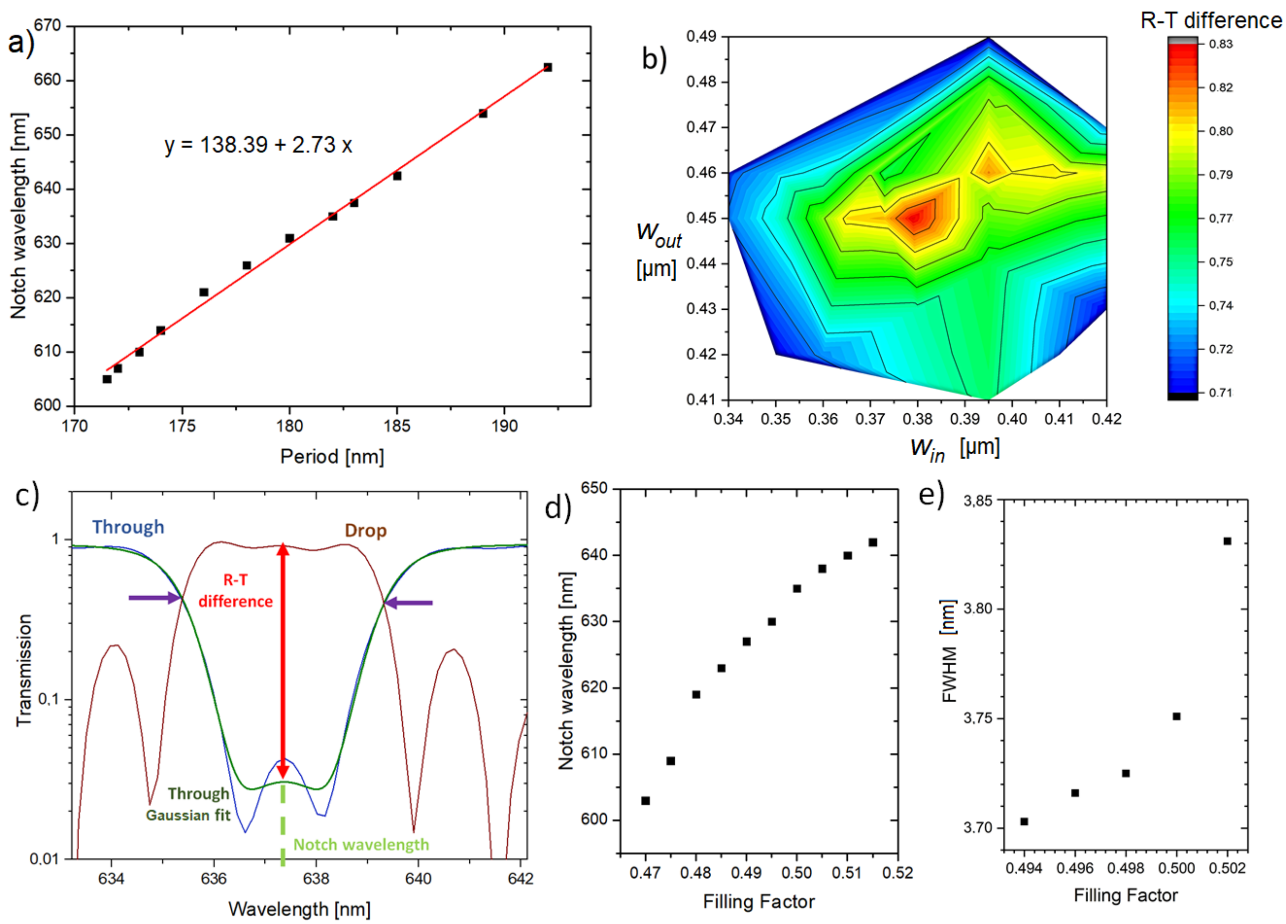

Figure 2. a) Dependence of the notch wavelength on the Bragg grating period obtained using MEEP and the linear approximation of the dependence. b) Color contour map for the dependence of the reflection-transmission difference on the widths of the waveguides. c) Transmission and reflection spectra approximated by the Gaussian fit. Full width and half maximum (FWHM) is shown. d) Dependence of the notch wavelength on the filling factor of the Bragg grating. e) Dependence of the FWHM on the filling factor.

4. Modeling

In the first step, we simulated the TE-mode field distribution for the Si_3N_4 waveguide on the SiO_2 layer in COMSOL Multiphysics, using Bragg waveguide cross-section. We observed the field distribution inside waveguide for two transverse electric modes (TE) and found effective mode indices (n_1 and n_2) for each of them. Using the obtained values and well-known Bragg equation (Shi et al., 2013), the Bragg grating period for operation at 637 nm wavelength with fixed 0.5 filling factor was estimated (Figure 1c).

In the second step, to obtain the spectral dependences of the transmitted and reflected light through the CDC, we used simulation in MEEP. We calculated transmission and reflection spectra for all the ports in order to obtain the most optimal parameters. For modeling, we chose resolution (number of pixels per micron) equals to 80 so that the computations would be precise enough compare to the operation wavelength. We used a top view 2D model of the CDC with perfect matched layer (PML) as the boundary conditions.

While looking for the most optimal parameters, each parameter was varied separately and after finding the most convenient one, it was fixed and then the next one was varied.

5. Results and Discussion

We started our study from the determination of the grating period and the initial value of the period was taken correspondingly to the Bragg condition. After varying the period, we obtained the linear dependence of the notch wavelength on the period (Figure 2a).

The growth rate of the central wavelength, depending on the grating period is equal to 2.7 and shown in Fig.2a by the red solid line. We obtained that the other performance, such as FWHM or the filtration depth didn't change significantly with respect to the period. For this reason, if another optimization parameter gave us better results, but shifted wavelength, we moved spectra back by tuning the grating period.

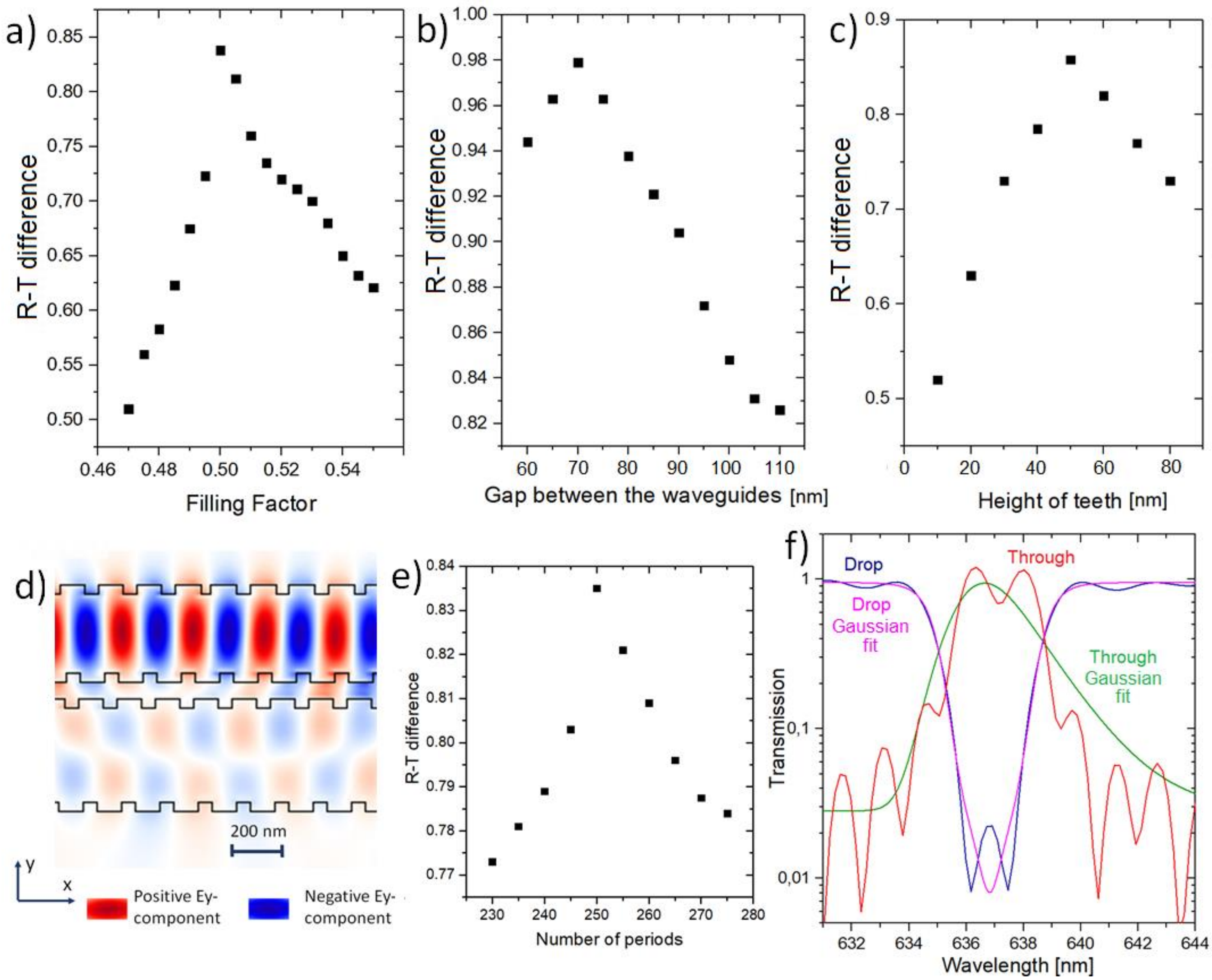

Figure 3. a) Dependence of the reflection-transmission (R-T) difference on the grating fill factor. b) Dependence of the R-T difference on the distance between the waveguides. c) Dependence of the R-T difference on the "teeth" height. d) Electric field distribution over the contra-directional coupler calculated using FDTD method in MEEP. e) R-T difference on number of periods dependence. f) Drop and through signals for the optimized contra-directional coupler at 637 nm operation wavelength.

Then we studied the model at the different widths of the waveguides. The difference between the normalized reflection and normalized transmission at the notch wavelength (R-T difference) was maximized. The greater the difference, the more filtered light directed to the output port relative to the non-transmitted (Figure 2c). Summarizing the calculation results we plotted the R-T difference using color contour map (Figure 2b), and found the output w_{out} = 450 nm, and the input w_{in} = 375 nm waveguide widths providing the R-T difference equal to 0.83.

Then we studied the dependence of the R-T difference (Figure 3e) on the number of periods and reached the value of 0.836 for the number of periods equal to 250.

The next parameter for the study was the dependence of the notch wavelength on the filling factor (Figure 2d). As the filling factor increases, the center wavelength also increases. At the same time, filling factor also influenced of FWHM (Figure 2e) and R-T difference (Figure 3a). We chose the filling factor providing maximum R-T difference in powers and the minimum FWHM simultaneously. The maximum R-T difference equals to 0.84 corresponds to filling factor of 0.5.

Also, we varied the height of the "teeth" in the corrugated Bragg waveguides. The maximum value of R-T difference equals to 0.86.

Therefore, using the numerical FEM and FDTD methods, we studied the electric field propagation filter. We found the geometrical parameters of the corrugated Bragg waveguide, which ensure operation at a wavelength of 637 nm with the maximum efficiency of reflected light relative to non-transmitted light. Such parameters include the number of periods N = 250, the input waveguide width w_{in} = 375 nm, the output waveguide width w_{out} = 450 nm, the gap g = 70 nm, the height of the Bragg's teeth h = 50 nm and the Bragg period Λ = 183.5 nm, FWHM = 3.703.

6. Conclusions

In this work silicon nitride contra-directional, using the numerical FEM and FDTD methods was studied. We found the geometrical parameters of the corrugated Bragg waveguide, which ensure operation at a wavelength of 637 nm with the maximum efficiency of reflected light relative to non-transmitted light. The number of periods N = 250, input waveguide width w_{in} = 375 nm, the output w_{out} = 450 nm, gap g = 70 nm, height of the Bragg's teeth h = 50 nm and the Bragg period Λ = 183.5 nm, FWHM = 3.703.

Further work will be devoted to the fabrication of the integrated filters and their experimental investigation.

Funding

The research was performed by support of Ministry of Education and Science of the Russian Federation (contract № 14.586.21.0063, unique identificatory RFMEFI58618X0063).

References

Aharonovich, I., et al. (2011) Diamond-based single-photon emitters. *Reports on Progress in Physics*, 74, 7.

Aspuru-Guzik, A. & Walther, P. (2012) Photonic quantum simulators. *Nat. Phys., 8,* 285–91.

Bahe, J. et al. (2009) A single photon source based on NV centers in diamond nanocrystals. *CLEO/Europe - EQEC 2009, 1.*

Boroojerdi, M. T., Ménard, M., & Kirk, A. G. (2016) Two-period contra-directional grating assisted coupler. *Opt. Express*, 24, 22865-22874.

Chuang, W., Huang, Y., Lin, H., & Lee, A. (2011) Fabrication of an asymmetric Bragg coupler-based polymeric filter with a single-grating waveguide. *Opt. Express*, 19, 10776-10788.

De Vos, K; Bartolozzi, I; Schacht, E; Bienstman, P. & Baets, R. (2007) Silicon-on-insulator microring resonator for sensitive and label-free biosensing. *Opt. Exp., 15,* 7610–7615.

Doerr, C. (2015) Silicon photonic integration in telecommunications. *Frontiers Phys., 3,* 37

Ferrari S.; Schuck C. & Pernice W. 2018 Waveguide-integrated superconducting nanowire single-photon detectors *Nanophotonics* 7 1725–58

Ghose, B., Krishnamurthy, C. V. & Rao, A. S. (2010) Two-Dimensional FEM Simulation of Ultrasonic Wave Propagation in Isotropic Solid Media using COMSOL. In *COMSOL Conference*, Bangalore.

Komrakova S.; Javadzade J.; Vorobyov V. & Bolshedvorskii S. (2019) CMOS compatible nanoantenna-nanodiamond integration *J. Phys. Conf. Ser.*

Malitson, I. H. (1965) Interspecimen comparison of the refractive index of fused silica, *J. Opt. Soc. Am.*, 55, 1205-1208.

Naghdi, B. & Chen, L. (2016) Silicon photonic contradirectional couplers using subwavelength grating waveguides. *Opt. Express*, 24, 23429-23438.

Nie, X., Turk, N., Liu, Z., & Baets, R. (2019). Grating assisted contra-directional filters with high rejection ratio in silicon nitride rib waveguides. *In 21st European Conference on Integrated Optics (ECIO 2019), Proceedings.* Ghent, Belgium.

O'Brien, J. (2007) Optical Quantum Computing. *Science, 318,* 1567–702.

Oskooi, A. F., at al. (2010) Meep: A flexible free-software package for electromagnetic simulations by the FDTD method. *Comput. Physics Communications*, 181, 687–702.

Okayama, et al. (2019) Asymmetric directional coupler type contra-directional polarization rotator Bragg grating: design. *Japanese Journal of Applied Physics*, 58, 6.

Philipp, H. R. (1973) Optical properties of silicon nitride. *J. Electrochim.*, 120, 295-300.

Silverstone, J. W., Bonneau, D., O'Brien, J. & Thompson, M. G. (2016) Silicon Quantum Photonics. *IEEE J. Sel. Top. Quantum Electron, 22,* 1–13.

Siregar, R. E., Bahtiar, A., Abrar, A. (2007) Study Of An Add-drop Filter Using A Single Bragg Coupler. *Bionatura*, vol. 9, no. 3.

Shi, W., et al. (2013) Coupler-apodized Bragg-grating add-drop filter. *Opt. Lett.*, 38, 3068-3070.

Shi W. et al. (2013d) Couplers for CWDM networks on silicon *Opt. Express, 21,* 6733–8

Soref. R. (2006) The Past, Present, and Future of Silicon Photonics. *IEEE J. Sel. Top. Quantum Electron, 12,* 1678-1687.

Topa, A. (2002) Contradirectional interaction in a NRD waveguide coupler with a metamaterial slab. *XXVII General Assembly of International Union of Radio Science (URSI GA'02).* Maastricht, The Netherlands, Aug. 17–24, 2002. CD Digest, paper no. 1878.

Wang, X.; Shi, W. & Chrostowski, L. (2013) Silicon Photonic Bragg Gratings in L. Chrostowski & K. Iniewski. High-Speed Photonics Interconnects (chapter 3). *Boca Raton, FL: CRC Press.*

Wang, X., Shi, W., Vafaei, R., Jaeger,N. A. F., & Chrostowski,L. (2011) Uniform and sampled Bragg gratings in SOI strip waveguides with sidewall corrugations. *IEEE Photon. Technol. Lett.*, 23, 290–292.

Yeh, P. & Taylor, H. F. (1980) Contradirectional frequency-selective couplers for guided-wave optics. *Appl. Opt., 19,* 2848–2855

Yves, J. St. *Contradirectional couplers as optical filters on the silicon on insulator platform* (Master's Thesis 2017) retrieved from https://corpus.ulaval.ca/jspui/handle/20.500.11794/27630

Zubkova, E., et al. (2018). Optimization of contra-directional coupler based on silicon nitride Bragg rib waveguide. *Journal of Physics: Conference Series*. 1124. 051048. 10.1088/1742-6596/1124/5/051048.